Chapter

Conversion of Gas Turbine Combustors to Operate with a Hydrogen-Air Mixture: Modifications and Pollutant Emission Analysis

Rafael Domingues and Francisco Brójo

Abstract

In this work, an overview of the use of hydrogen in aviation, the modifications needed to adapt an existent gas turbine to use hydrogen, and a CFD simulation of an existent gas turbine burning hydrogen are performed. The CFD simulation was done in a CFM56-3 combustor burning hydrogen and Jet A. It was intended to evaluate the viability of conversion of existent gas turbines to hydrogen, in a combustion point of view, by analyzing the emissions while burning it through ICAO's LTO cycle. The pollutant emissions (only NOx, since hydrogen combustion produce only water vapor and NOx) were evaluated through a detailed mechanism and the Ansys Fluent NOx model to get a better agreement with the ICAO's values. For this assessment, several sensibility studies were made for hydrogen burn, for example, the analysis of the air flow with/without swirl in the primary zone and different inlet temperature and pressure for fuel. In the end, it was concluded that theoretically the CFM56-3 combustor can be converted to operate with hydrogen fuel with minor changes (related to injection system). The quantity of NOx produced for each power setting when burning hydrogen is expected to be almost twice the values for Jet A.

Keywords: CFM56-3, combustion chamber, pollutant emissions, jet fuel, hydrogen fuel

1. Introduction

The sustainable growth of aviation is important for the future of the economic growth, development, commerce, cultural exchange, and many other factors. According to some experts, by 2045, international air traffic is expected to increase by 3.3 times [1]. In 2015, international aviation consumed approximately 160 megatons (Mt) of fuel. By 2045, compared with the anticipated increase of 3.3 times growth in international air traffic, fuel consumption is projected to increase by 2.2–3.1 times

IntechOpen

compared with 2015, depending on the advances in technology and the Air Traffic Management (ATM) scenario [1].

The emissions resulting from the combustion of fossil fuels are usually considered as the main responsible for Greenhouse Gas (GHG) emissions, which are pointed as the primary factor that leads to global warming. For climate change, the primary concerns are emissions of CO, CO_2, NOx, and nvPM [2]. Also of concern are persistent contrails, which lead to cirrus clouds. Generally, it is the combination of a number of factors that determine the overall impact of the emissions on global surface temperature over a given timescale. These factors consist of quantities emitted, residence time, radiative forcing, and the temperature response profile of a particular pollutant [2].

The CO_2 emissions are of particular concern because of its exceptionally long residence time (thousands of years). Aviation today accounts for 2–3% of global CO_2 emissions. While at the global level, CO_2 emissions are increasing by around 3% per year, aviation's emissions covered by the EU ETS have increased on average by 5% year-on-year between 2013 and 2018. By 2040, it is expected that international aviation emissions could rise by up to 150% compared with 2020. These growth forecasts take into account the incremental technology improvements that may reduce fuel consumption and emissions by 1–1.5% annually [3].

About the NOx emissions, they are evaluated in two possible scenarios, which are landing and take-off (LTO) NOx emissions, which primarily affect local air quality, and full-flight NOx emissions, which have more effect on the global climate. In 2015, LTO NOx emissions were approximately 0.18 Mt., and by 2045, they are projected to range from 0.44 to 0.80 Mt. depending on the technology and ATM scenario [1]. While, in 2015, the full-flight NOx emissions of international aviation were 2.50 Mt., by 2045, the full-flight NOx emission projection ranges from 5.53 to 8.16 Mt., which represents a 2.2–3.3 times growth compared with 2015 [1].

To mitigate this problem, there are several possible solutions. On the one hand, the fuel burn reductions through the upgrade of the technology employed in the actual aircrafts such as the airframes (aerodynamics and mass) and the engines, both with the aim of achieve higher efficiency [2]; on the other hand, the use of alternative fuels and power sources [4, 5]. According to the ICAO 2016 trends assessment, a 100% substitution of aviation fuel with SAF could reduce 63% of the baseline CO_2 emissions from international flights in 2050 [4]. As referred by ATAG [5], it is possible that aviation meets net-zero CO_2 emissions by 2050; however, it would take an enormous effort to make it a reality. This would mean a rapid and massive transformation on aviation's energy supply through the use of SAFs, and it would require acceleration in aircraft and engine technology development, mainly: electric-, hybrid-, and hydrogen-powered aircraft.

Within this context, the conversion of the current gas turbine engines to new sustainable fuels can also be a solution. So, in this study, be analyzed the feasibility of the use of hydrogen fuel as substitute of the conventional jet fuel in a CFM56–3 combustor using a CFD approach. The NOx emissions produced while completing the ICAO's LTO cycle burning this fuel will be assessed for the standard operating conditions of the engine, as well as the influence of several operating parameters (swirl effect, temperature, and pressure of fuel) in these emissions.

1.1 Brief historical review

To date, the largest user of hydrogen in aeronautics is the space program where it is used as fuel for the rocket engines of launch vehicles. The first successful launch of a space vehicle propelled by a liquid hydrogen/liquid oxygen rocket engine took place at

Cape Kennedy on November 27, 1963. Several other rocket engine manufacturers in the United States were involved in the development of designs using LH_2; for example, the General Electric Company, the Rocketdyne Division of North American Aviation (now Rockwell International, Inc.), and the Aerojet General Corporation were among the leaders. Of the designs developed by these companies, the Rocketdyne J2 engine is an example, which has been eminently successful. It was used in both the second and third stages of the Saturn V launch vehicle, used in the Apollo program, which landed U.S. astronauts on the moon. In all of the launches of the Apollo program, there has never been a failure of one of the hydrogen-fueled rocket engines.

However, the space applications are relatively recent, if we look at history, the first reported use of hydrogen in aeronautics was a long time ago. According to Brewer [6], hydrogen was first employed as lifting medium when, in France, a small silk balloon was constructed by the Roberts brothers, under the direction of physicist J.A.C. Charles, and it was flown in Paris on August 27, 1783. This balloon rose to a height of 3000 ft. (914.4 m) and traveled a distance of 15mi (24.14 km). In that year, on December 1, a larger hydrogen-filled model, which carried two passengers, the physicist Charles and one of the Roberts brothers, was launched. This flight traveled 25mi (40 km) from Paris in less than 2 hours.

Later in history, airships came into being as a result of man's desire to control the direction and speed of flight. Numerous attempts were made to achieve such control with balloons without measurable success until 1852, when a Frenchman, Henri Giffard, constructed an airship on which he mounted a steam engine of his own design. Giffard flew this hydrogen-filled airship from the Hippodrome in Paris on September 24, 1852, attained an estimated speed of 6 mph, and demonstrated the first appreciable control of a "lighter-than-air craft." In 1872, Paul Haenlein developed and flew an airship powered by an internal combustion engine, which was fueled by gaseous hydrogen that was drawn from the lifting cells of the airship envelope [6]. A significant step leading to the use of hydrogen in commercial air transportation occurred in 1900 when the first rigid airship designed by Count Ferdinand von Zeppelin, the LZ-1, made a successful flight. In 1911, commercial air operations were started by a German transportation company (DELAG), using five Zeppelin airships. In October 1924, the Zeppelin factory at Lake Constance, in Germany, completed the construction of the LZ-126, inflated it with hydrogen, and delivered it to the United States by a transatlantic flight.

In 1955, a report by Silverstein and Hall of the (then) NACA-Lewis Flight Propulsion Laboratory was published in which the potential of liquid hydrogen as a fuel for use in both subsonic and supersonic aircraft was explored. According to it, theoretically, the use of hydrogen fuel could significantly improve the maximum range [6]. As a result of this study, an experimental program with a U.S. Air Force B-57 twin-engine medium bomber was initiated to demonstrate the feasibility of burning hydrogen in a turbojet engine at high altitude. The modified aircraft was first flown in 1956.

From 1954 to 1955, Lockheed Aircraft Corporation made a series of conceptual design studies of hydrogen-fueled aircraft in cooperation with Pratt & Whitney Aircraft and the Rex Division of AiResearch Corporation. In 1956, the U.S. Air Force awarded a contract to Lockheed's Advanced Development Projects organization to build two prototype aircrafts (known as CL-400), which would be capable of cruising at Mach 2.5 at 100000 ft. (30,480 m) altitude. This aircraft was to carry a two-man crew, and the main objective was related to long-range reconnaissance missions.

Also in 1956, at the same time the U.S. Air Force contracted with Lockheed for the development of the CL-400 airplane, and the Pratt & Whitney Aircraft Division of United Aircraft Corporation was awarded a contract to investigate the feasibility of using LH_2 as a fuel in aircraft engines. The work at Pratt & Whitney covered a broad spectrum ranging from applied research efforts such as heat transfer and materials investigations, to development testing of a J57 engine modified to operate on LH_2. It also included the design, construction, and test of a new design of engine (the Model 304). Conversion of the J57 to operate on LH_2 was accomplished in just 5 months, and the first tests were performed in the fall of 1956 [6]. The work with the J57 showed that conventional jet engines could be readily adapted to use LH_2 fuel. In this research, after examining many possible cycles, the Hydrogen Expander cycle (this cycle is well explained by Brewer [6]) was selected for experimental evaluation to create the Model 304 engine. This was a unique cycle developed specifically to take advantage of the properties of hydrogen and to meet the performance requirements of the CL-400 airplane. The first demonstration test of a complete 304 engine was accomplished in September 1957.

In spite of the success in developing practical solutions to the problems encountered with handling the cryogenic liquid fuel, the CL-400 aircraft was never built due to performance and logistics limitations. So, in 1957, the program was terminated by mutual agreement between the Air Force, Lockheed, and Pratt & Whitney. However, the CL-400 design and development program showed that it was entirely feasible to build a hydrogen-fueled airplane.

In the 1970s, Lockheed performed studies on different liquid hydrogen-fueled subsonic cargo and passenger transport jets for NASA Langley Research Center. The results are presented in the NASA-reports NASA CR-132558, NASA CR-132559, and NASA CR-144935. The main conclusions from these and furthers studies have been summarized by Daniel G. Brewer in [6]. The studies showed that hydrogen propulsion is especially beneficial in terms of energy use for long-range aircraft with internal hydrogen tanks.

In the 1980s, Tupolev developed the Tu-155 that was based on the medium-range transport aircraft TU-154B. Moreover, the TU-155 was built and successfully tested without any serious incidents, and it first flew burning hydrogen in one of its three engines in April 1988. The modified engine was also able to be run with natural gas. The TU-155 was followed by the TU-156 that could be run with natural gas or kerosene [7].

At the beginning of the twenty-first century, the Cryoplane Project comprised of 36 European research partners from industry, universities, and research institutions. They contributed to this project covering aircraft configuration, systems and components, propulsion, safety, environmental compatibility, fuel sources and infrastructure, transition. The total project time was 26 months and started in April 2000. During this project, several conventional and unconventional overall aircraft design studies and detailed investigations of hydrogen fuel systems and components were performed [7, 8].

More recently, in July 2010, Boeing unveiled its hydrogen-powered Phantom Eye UAV that uses two converted Ford Motor Company piston engines. Nowadays, governments and companies are investing again in hydrogen's potential. For instance, the ENABLEH2 (ENABLing cryogEnic hydrogen-based CO_2 free air transport) consortium was given such a hand, almost 20 years after the European Commission's last attempt to ramp up LH_2 research and development under the Cryoplane project. The project's objective is to demonstrate that switching to hydrogen is feasible and must

complement research and development into areas such as advanced airframes, propulsion systems, and air transport operations [9]. Another example is the project named ZEROe, announced by Airbus in September 2020, which has the ambition to develop the world's first zero-emission commercial aircraft. This project consists of the development of three concept planes (powered by hydrogen combustion through modified gas turbine engines or hybrid systems), which Airbus says that could be ready for deployment by 2035 [10].

2. Basic engine principles

2.1 CFM56-3 general specifications

The CFM56-3 is a high bypass, dual-rotor (or dual-shaft), axial flow turbofan engine, and this particular variant of CFM56-3 has a bypass ratio of 5.1:1 and a dry weight of 1966 kg [11, 12]. Its dual-shaft design consists of a fan and booster (low-pressure compressor), high-pressure compressor, annular combustion chamber, and a high- and low-pressure turbine section. The two shafts respectively connect the low- and high-pressure sections using a five-bearing system (three roller, and two ball bearings) [13].

2.2 Combustor

First of all, it is important to understand the difference between the combustor and the combustion chamber [14]. The combustor includes all of the combustion systems, that is, the diffuser, the combustion chamber, the inner and outer casing, the spark plugs, and the fuel injectors, whereas the combustion chamber refers to the exact place in which combustion takes place.

The main purpose of a gas turbine combustor is to introduce heat energy into the mass of air previously compressed (in the compressor) [15], by burning fuel in it so that the products of combustion can be expanded to get useful work output (absorbed by the turbines) and then, on their discharge to atmosphere, provide a propulsive jet [16]. Due to space limitations and requirements of energy and momentum, the volume flow rate as well as rate of heat release is very high in a gas turbine combustion chamber and the residence time of fuel is very small, of the order of a few milliseconds [15]. In gas turbines, the combustion is a continuous process that takes place at high pressure in a smaller space and usually at a very high temperature [16]. Thus, continuously high combustion temperatures, large continuous flow, and high heat energy release make the design and development of a gas turbine combustor rather difficult [15].

A gas turbine combustor must satisfy a wide range of requirements. However, for the aircrafts, the priorities are the reliability, the low fuel consumption, low pollutant emissions, engine size, and weight [17].

The choice of a particular combustor type and design is determined largely by the overall engine design and by the need to use the available space as effectively as possible [16]. Overall, the combustors may be subdivided into three main types: tubular or can, tubo-annular, and annular [16]. The CFM56-3 has an annular combustor, and **Figure 1** shows it during the digitalization process to obtain the model of geometry used in this work.

The annular configuration is used by most modern jet engines because of its lighter design. This type of combustor represents the ideal configuration for combustors since
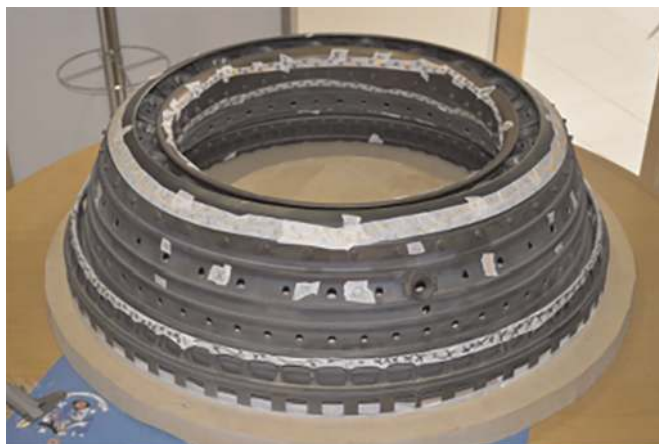
Figure 1.
CFM56-3 combustor photograph [14].

its "clean" aerodynamic layout results in compact dimensions [16]. This configuration consists of an annular liner that is mounted concentrically inside an annular casing. Among the advantages, the annular combustion chambers have the least pressure drop due to larger volume per unit surface area and are more efficient than can-type chambers. It also requires about half of the diameter of can-type chambers for the same mass flow [15].

Its main drawback stems from the heavy buckling load on the outer liner [17]. Moreover, any change in the flow velocity profile can result in significant change in the temperature distribution of the outlet gases, and distortion of inner annular chamber is critical because it disrupts the flow of cooling air and also changes the outlet temperature distribution. This is because of lower degree of curvature of the chamber surfaces [15]. Another drawback is related to experimental tests of this type of combustion chamber. At full-load conditions, the tests of large annular combustion chambers supplying air at the levels of pressure, temperature, and flow rate required are extremely difficult, and the cost is very high [17]. Nowadays, there are very few facilities worldwide that can supply air in those conditions [18].

3. Fuels in gas turbine engines

At the current time, almost all aviation fuel (jet fuel) is extracted from the middle distillates of crude oil (kerosene fraction), which distils between the gasoline and the diesel fractions [18]. The Jet A and Jet A-1 grades are the most used kerosene-type fuels worldwide in civil aviation.

As referred before, to mitigate the problem of the pollutant emissions in the future, there seem to be two viable solutions, the use of SAFs or the use of hydrogen fuel (through hydrogen combustion engines or fuel cells). In this work, will only be considered the hydrogen for the combustion gas turbine engines (GTEs).

3.1 Hydrogen

The hydrogen is the simplest and most abundant of the chemical elements in the universe. On Earth, under standard conditions (H_2), its concentration is negligible. However, in chemically combined form, it is the third most abundant element on

Earth. Consequently, hydrogen can be considered an energy carrier, similar to electricity, since it can be produced from other compounds, mostly from hydrocarbons and water [19]. The main reasons why hydrogen can play an increasingly significant role in meeting the worlds energy demands and addressing environmental concerns are that hydrogen meets three important criteria: a promising low-carbon alternative reducing emissions of GHG, providing energy security, and the possibility of reducing local pollutants, that is, NOx and particulates [19].

On a commercial scale, despite the several production sources, most of the hydrogen is currently produced through the process of steam reforming of methane (SRM) from natural gas [19]. As part of the energy future, the various hydrogen sources can be grouped into three types, namely fossil fuels (coal, natural gas, petroleum, oil shale, etc.), renewable sources (biofuels, water, photovoltaic, solar, algae, etc.), and nuclear (e.g., using thermal energy from nuclear reactions for water splitting). For hydrogen to be part of a sustainable energy future, renewable and nuclear sources need to play a more significant role in hydrogen production, and cost-effective carbon capture and storage technologies need to be developed and upgraded.

3.2 Utilization of hydrogen in gas turbine engines

For the use of the hydrogen fuel in the current GTEs, in theory, the minimum modifications needed are the change of the injection system and the implementation of facilities to evaporate the hydrogen, which is stored in the tanks in a liquid (or cryogenic) state. This can be accomplished by an external heat source or a heat exchanger (HE) [20]. However, to take full advantage of the hydrogen's distinct thermo-transport properties (high diffusivity, low ignition energy, wide flammability limits, and the highest laminar flame speed) that make its combustion and emission characteristics notably different from those of hydrocarbons fuels, beyond the injection system, the combustion chamber must be also changed [19]. In **Table 1**, is provided a comparison between the main properties of hydrogen and Jet A [6, 9].

When changing to hydrogen, either the combustor outlet temperature (COT) or the net thrust could be retained [20]. Because of the considerably higher heating value of hydrogen, the fuel flow to achieve the same COT or net thrust is reduced by almost

Properties	Units	H2	Jet A
Liquid density	g cm^{-3}(at 283 k)	0.071	~0.811
Melting point	K	14.01	−263
Boiling point	K (at 1 atm)	20.27	440–539
Heat of vaporization	J g^{-1} (at 1 atm)	446	360
Specific heat	J g^{-1}	9.69	1.98
Lower heating value	MJ kg^{-1}	119.96	43.15
Flammability limits in air	vol%	4.0–75.0	0.6–4.7
Thermal energy radiated to surrounding	%	17–25	30–42
Diffusion velocity in NTP air	cm s^{-1}	≤2.00	<0.17
Flame temperature in air	K (stoichiometric)	2318	2200

Table 1.
Properties for hydrogen fuel and Jet A fuel.

two-thirds. When the COT is preserved, the net thrust increases, resulting in a corresponding increased specific thrust. When it is opted to retain the net thrust, this results in a lower COT [20]. According to Boggia and Jackson [21], the performance improvements could be explained by two fundamental changes when using hydrogen: reduced mass flow and changed composition of the gases expanding through the turbine(s). While the latter improves the performance, the former deteriorates the performance. Reduced mass flow through the turbine lowers the thrust output for two reasons. First, decreasing the fuel flow implies that the exhaust mass flow decreases accordingly; hence, without any variation in gas composition, the thrust output decreases. In second, a reduced mass flow through the turbine will result in a higher total temperature drop and, thereby, also a higher total pressure drop across the turbine in order to deliver the same amount of power to the compressor. Because of the lower total temperature and pressure at the turbine exit, both the pressure thrust (thrust due to different pressure at engine inlet and exit) and momentum thrust decrease (the effect of decreased core nozzle velocity).

However, the loss in thrust due to reduced mass flow is offset by the increased thrust owing to changed properties of the combustion products [21]. With the use of hydrogen, the combustion products contain no CO_2 and a larger portion of H_2O, which has a higher C_p value than CO_2. Having investigated a simple turbojet engine, Boggia and Jackson [21] concluded that the C_p value has increased by $\sim$4% in the hot section of the engine when changing to hydrogen fuel. Increased C_p value through the turbine will similarly, but in the opposite direction as reduced mass flow, affect the performance. For a fixed power output, it will cause smaller total temperature and pressure drops across the turbine. Provided that the core nozzle is not choked, a larger nozzle expansion ratio will result in a larger exhaust velocity, which, in turn, will increase the momentum thrust. In total, the positive effect of increased C_p value outweighs the effect of reduced mass flow and, hence, results in an increased net thrust when switching to hydrogen and retaining the COT [20].

It should be pointed out that the energy consumption to attain a certain COT is highly dependent on the fuel-injection temperature and the location of the heat exchanger (HE) used to evaporate the liquid hydrogen. By heating the fuel more, it is possible to achieve performance benefits. The effects on engine performance are quite small, but still there are some desired features that could be exploited [20].

If the COT is kept the same, the turbine entry temperature (TET) is also about the same, thus requiring the same cooling technology [21]. On the other hand, the option of lowering the COT to preserve the net thrust will lead to a decrease in TET. So, this will require less advanced cooling technology as well as having a favorable effect on turbine blade life. Moreover, designing for a lower maximum cycle temperature will help to suppress the NOx emissions.

3.3 Mechanisms of pollutant formation

The concentration level of pollutants in gas turbine exhaust can be related directly to several factors that control the emissions in conventional combustors. These factors may be considered in terms of primary-zone temperature, equivalence ratio, degree of homogeneity of the primary-zone combustion process, residence time in the primary zone, liner-wall quenching characteristics, and fuel spray characteristics [17]. These factors vary from one combustor to another and, for any given combustor, with changes in operating conditions [17].

For the conventional fuels, such as hydrocarbons (in this case Jet A) or even the SAFs, the pollutant emissions of most concern are CO, CO_2, UHC, NOx, and PM (or smoke). From the environmental standpoint, hydrogen is nearly a clean fuel once it produces only NOx (considering that water vapor is not a major pollutant) [19]. So, in this work, only the NOx emissions will be presented.

About the NOx (NO plus NO_2 emissions), in conventional gas turbine combustors, there are four main mechanisms that are responsible for the NOx formation: thermal NO, nitrous oxide (N_2O) mechanism, prompt NO, and fuel NO. The last one is usually of less importance for normal fuels (there is no fuel-bond nitrogen) [17]. In the case of hydrogen burn, we must still consider the NO formation through intermediate NO_2 [19].

For hydrocarbon fuels, the two main mechanisms that are responsible for the formation of NOx are thermal NO and prompt NO, while for hydrogen flames the two main mechanisms associated with NOx formation are the thermal NO and NO formation through intermediate NO_2. So, in this subsection only these three mechanisms will be referred. For more information about the others, there are a good review of them in Lefebre et Ballal and Kenneth Kuo [17, 22].

The thermal NO is produced by the oxidation of atmospheric nitrogen (N_2) in high-temperature regions of the flame and in the post-flame gases [22]. This endo-thermic process is controlled largely by flame temperature, and it proceeds at a significant rate only at temperatures above around 1850 K (it requires the breaking of the tight N_2 bond) [17, 19, 22]. For the typical conditions encountered in conventional gas turbine combustors (high temperatures for only a few milliseconds), NO increases linearly with residence time, but does not attain its equilibrium value. The extended Zeldovich mechanism is utilized by the most of the proposed reaction schemes for thermal NO. The principal reactions of this mechanism are represented in Eqs. (1)–(4) [17, 19]:

$$O_2 \rightleftharpoons 2O \tag{1}$$

$$N_2 + O \rightleftharpoons NO + N \tag{2}$$

$$N + O_2 \rightleftharpoons NO + O \tag{3}$$

$$N + OH \rightleftharpoons NO + H \tag{4}$$

The prompt NO can be formed in a significant quantity in some combustion environments such as in low-temperature, fuel-rich conditions and when residence times are short. These conditions can be created in gas turbines [18].

In hydrocarbon flames, prompt NO occurs in the earliest stage of combustion and its formation is associated with the reaction of molecular N_2 with radicals, such as C, CH, and CH_2, which are fragments derived from fuel, through a complex series of reactions and many possible intermediate species. Some of these reactions are represented in Eqs. (5)–(9):

$$CH + N_2 \rightleftharpoons HCN + N \tag{5}$$

$$N + O_2 \rightleftharpoons NO + O \tag{6}$$

$$HCN + OH \rightleftharpoons CN + H_2O \tag{7}$$

$$CN + N_2 \rightleftharpoons NO + CO \tag{8}$$

$$CH_2 + N_2 \rightleftharpoons HCN + NH \tag{9}$$

For hydrocarbon flames, the major contribution is from CH and CH_2 species, as shown in Eqs. (5) and (9). The products of these reactions could lead to formation of amines and cyano compounds that subsequently can react with species such as N, O, or OH to form NO by reactions like those occurring in oxidation of fuel nitrogen or oxidation of other nitrogen species. At present, the prompt NO contribution to total NOx from stationary combustors is small. However, as NOx emissions are reduced to very low levels by employing new strategies that tend to reduce the flame temperature (such as burner design or geometry modification), the relative importance of the prompt NO can be expected to increase [18].

For hydrogen flames, the second mechanism that is relevant for the NOx emissions corresponds to the NO formation through intermediate NO_2. This mechanism may be represented by the **Eqs. (10)** and **(11)** [19]:

$$NO + HO_2 \rightarrow NO_2 + OH \tag{10}$$

$$NO_2 + H \rightarrow NO + OH \tag{11}$$

3.4 Influence of temperature/pressure in NOx formation with hydrogen fuel

Owing to its high adiabatic flame temperature, hydrogen combustion produces significant NOx. Therefore, by increasing the strain rate (a_s), which is pressure-dependent, the flame temperature can be lowered and NOx emissions are reduced. So, the pressure can be also a controlling parameter for NOx formation with hydrogen flames.

This way, the thermal NO mechanism is dominant at low pressures, whereas NO formation *via* intermediate NO_2 becomes important at moderate pressures once in that condition, the flame temperature decreases for a given strain rate, a_s, due to enhanced recombination by the reaction [19]:

$$H + O2 + M \rightarrow HO2 + M \tag{12}$$

Consequently, the maximum NO formation decreases for moderate pressures [22].

At higher pressures, the net effect of reactions (10) and (11) is to H + $HO_2 \rightarrow$ 2OH, through which radicals H, OH, and O are produced [19]. This enhances the formation of thermal NO. Some studies refer that under specific conditions, the formation of NO can be dominant over NO_2.

Still considering the influence of pressure, but now for hydrocarbon fuels, the N_2O and prompt mechanisms dominate at low temperature and are independent of pressure, whereas the higher NOx levels associated with higher combustion temperature are primarily due to thermal NO, which exhibits a square-root dependence on pressure [22].

3.5 Chemical kinetic mechanisms

Chemical kinetics is a capital point when modeling a combustion problem. In this case, the fuel combustion kinetics is extremely important in order to develop a model that allows a good emission prediction from the engine. Without proper kinetics all the attempts will go in vain. The development of detailed chemical kinetic models is extremely challenging once typical fuels (such as gasoline, diesel, and jet fuels) derived from different sources can be composed of hundreds to thousands of compounds. Therefore, detailed kinetic models for such fuels cannot contain all the compounds due to the limitation of current computational resources [23]. For that reason, a simplified mixture called surrogate mixture must be defined and used to develop a kinetic model.

For the emission predictions, the kinetic model development can be even more diffi-cult once the NOx chemistry must be developed together with fuel chemistry making realistic chemistry getting even more complicated. In this section, will be introduced the Jet A and hydrogen combustion kinetic models applied in this study.

3.5.1 Jet A kinetic mechanisms

Although kinetic models of jet fuel are still underdeveloped, significant progress has been made in this area in the recent decades. Jet fuels are kerosene-type cut of petroleum containing C-10–C-18 hydrocarbons, including alkanes, cycloalkanes, and aromatic compounds. The literature reviews show that there are several kinetic models available for jet fuel combustion and some of these models are listed (and briefly descripted) by Mostafa [23].

However, only few of them are suitable to satisfy our current needs. Based on our objective to predict aircraft engine emission (specifically NOx) using CFD simulation, we need at first a jet fuel kinetic mechanism that allows to simulate the combustion process and, then, one that fairly predicts NOx formation in this combustion chamber. As CFD with kinetic models is computationally highly expensive, the number of species in the kinetic scheme needs to be limited. For that reason, after evaluating the kinetic models available, it was opted by the option presented by Kundu et al. [24].

Kundu et al. [24] proposed a simplified kinetic mechanism with NOx chemistry based on 17 species and 26-step reaction for Jet A (17 steps for Jet A reaction and nine steps for the sub-mechanism for NOx prediction). This mechanism has been devel-oped specifically to predict NOx formation during combustion of aviation kerosene. However, the mechanism does not cover the entire range of pollutant species, once to limit the number of species, the mechanism does not include NO_2. Despite the limita-tion of this kinetic model, it was used in this work. This was not the best option, but among the available ones was the least bad.

3.5.2 Hydrogen kinetic mechanisms

The hydrogen oxidation chemistry represents the most fundamental and impor-tant building block in the hierarchy of hydrocarbon chemistry. Consequently, its chemistry has been extensively investigated, and a large number of detailed mecha-nisms (that can be found in the literature), including H_2/O_2 kinetics, have been developed and validated using different combustion configurations [19, 25]. Some of these mechanisms have been optimized for the combustion of pure hydrogen, but most of them are dedicated to the combustion of hydrocarbons including sub-mechanisms for H_2/O_2 chemistry. However, the accuracy of the H_2/O_2 subset is also essential for the overall performance of a hydrocarbon mechanism [19].

To choose the kinetic model more adjusted for this case, some reviews available in the literature [25, 26] were analyzed. For instance, Ströhl et al. [25] made an evalua-tion of detailed reaction mechanisms for hydrogen combustion under gas turbine conditions. That study shows that the mechanisms of Li et al. or Ó Conaire accurately represent H_2/O_2 kinetics under gas turbine conditions. However, it suggests that the Li et al. mechanism is best suited for the prediction of H_2/O_2 chemistry since it includes more up-to-date data for the range of interest [25]. Also, the Li et al. mechanism has been found to provide the best match with measurements over a wide range of equivalence ratio and pressure, using various targets, including shock tube ignition delay and laminar flame speed data [26].

So, it was concluded that the Li et al. mechanism should perform better than the others, and for that reason it will be used in this work. For the NOx prediction (of hydrogen burn), was used the NOx sub-mechanism based on the study by the Glarborg group that is available in the database of ANSYS Fluent 2020R2 together with the mechanism of Li et al.

4. Materials and methods

4.1 Geometry

For this study, was used a CAD design of the CFM56–3 combustor made in the study [14], based on the CFM56-3 combustor of **Figure 1**. Due to the existent symmetry in the CFM56-3 combustor and in order to decrease the simulation time and effectively represent the four fuel injectors (in the 20) that supply a richer mixture, it will be used only a quarter section of the combustor for simulation purposes; that is, there will be one fuel injector for every five injectors present in each quarter section of the model combustor that supplies an even richer mixture. In this study, the rich fuel injector is the middle one (element 24 of the **Figure 2b**). All the details present in the combustor geometry are represented in **Figure 2**, including the combustor walls, dome, dilution holes, fuel injectors, and primary/secondary swirlers.
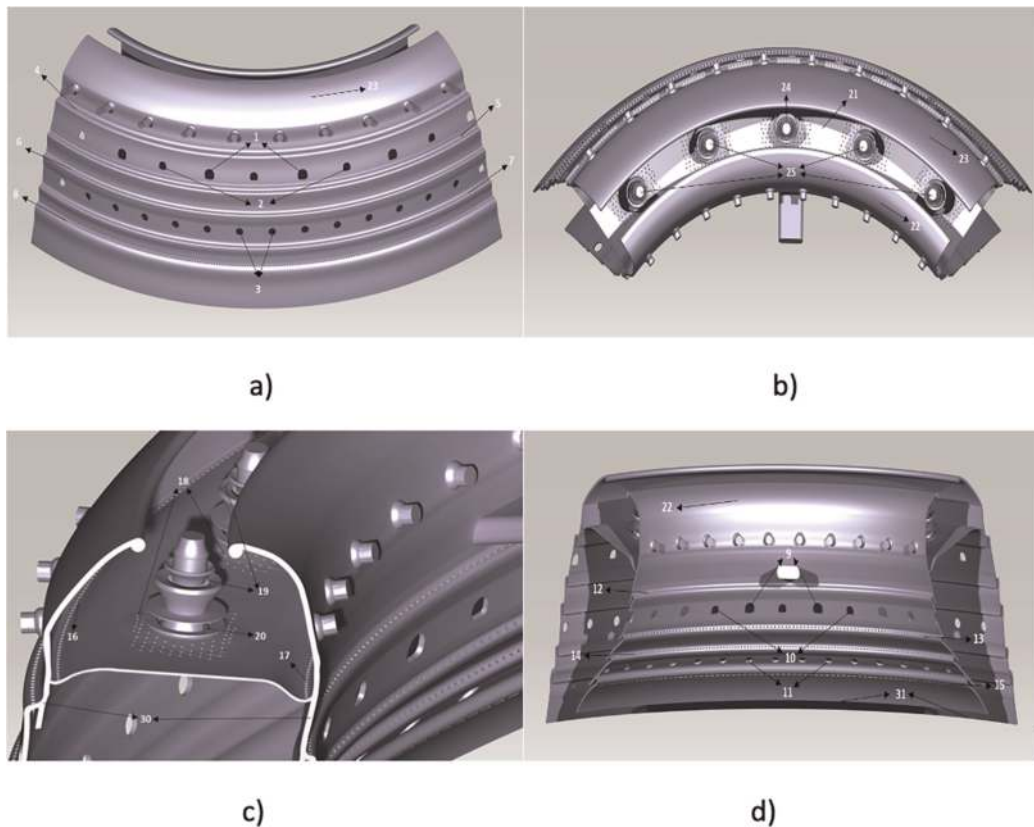

Figure 2.
Views of the CAD combustor model section used in the simulations: (a) outside view; (b) top view; (c) side view; and (d) inner view.

4.2 Modifications in the original geometry

As told by Oliveira [14], there were some parts of the combustor such as the swirlers that the exact geometry was not achieved. Furthermore, after analyzing some documentation of the CFM56-3 engine, photos of the combustor and doing the preliminary simulations, there were found some problems related with the fuel injectors position, the shape of the exit of the secondary swirlers, and the connection of this exits with the cooling walls of the dome. All of these problems were affecting the results. For that reason, some changes have been attempted to try to correct these small problems. All the changes in the model were performed in CATIA V5 R20. In **Figure 3** are presented two cut-view images of the first swirler, in which the first shows the original CAD model received and the second the final CAD model with the modifications made during this work.

During the early phases of the work, it was concluded that even so, the simulation time for the quarter section would be very large. So, to test new sets of modifications needed in the geometry, mesh, or the used models, a geometry where only one injector was represented was developed. Thereby, some sets of modifications could be excluded without spending the total time of the simulation in the quarter section.

4.3 Mesh generation

In this work, several meshing software (HELYX-OS, SnappyHexMesh, Simscale and Fluent Meshing) were tried in order to get the best mesh possible with the computational resources available (mainly the quantity of RAM). Due to the complexity of the geometry, the only software that provided a good quality mesh was the Fluent Meshing after using the set of tips provided by ANSYS in [27] about the best practices for gas turbine combustion meshing. This way, it was possible to create a good enough mesh for the simulation, where all the features of the geometry were correctly represented with the available computational resources.

After analyzing several meshes, the independency test was performed using three meshes, with coarse, medium, and fine refinement, having 11,830.638 cells, 16.318.327 cells, and 22.602.875 cells, respectively. The data collected relative to numerical/experimental data for Jet A fuel (no experimental data relative to H_2 combustion in this GTE was available) were presented by Ribeiro [28] and ICAO [12], and

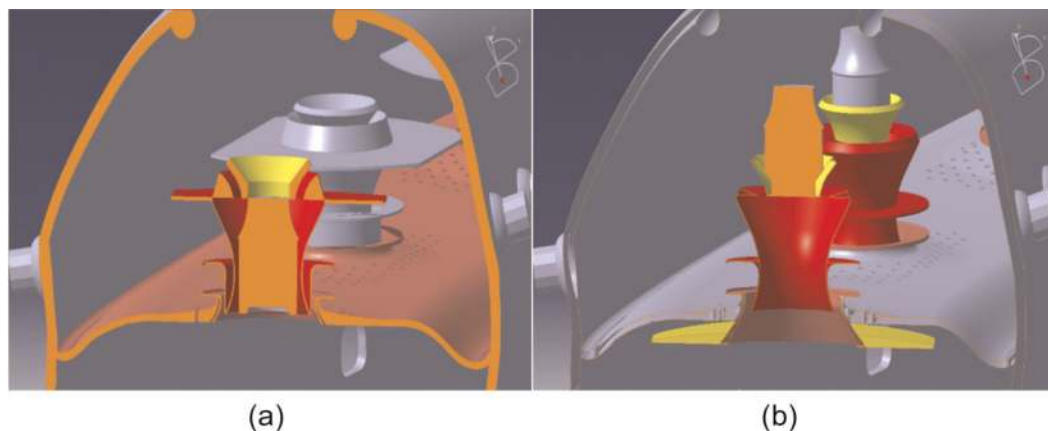(a)   (b)

Figure 3.
Cut view of the models: (a) original model and (b) modified model.

these documents contain the exit temperature of the combustion chamber (only for the operating condition of 100%) and the NOx emissions of the engine, respectively. For that reason, the parameters used to analyze the independency of the mesh were:

- The average static temperature of the combustion chamber in the outlet;

- The average static temperature and velocity in a defined plane (cut-view of the first swirler), once the NOx emissions depend mainly of the temperature and residence time inside the combustion chamber.

All the independency tests were performed for the operating condition of 100%, since it is the only operating condition where the outlet temperature of the chamber is known. The maximum difference occurred for the average static temperature in the plane of the cut view of the swirler, and it was in the order of 2.16% between the values of the coarse and the intermediate meshes; however, between the values of the intermediate and the fine meshes, the difference was only 0.1%. The difference between the values of the average static temperatures for the outlet was nearly 0% between the coarse and the intermediate meshes as well as between the intermediate and the fine meshes. For the velocity magnitude, in the cut-view plane, the difference between the values was approximately 0.71%, between the values of the coarse and intermediate meshes, and 0.49%, between the values of the intermediate and the fine meshes.

4.4 Numeric simulation

The software used to perform this study was ANSYS Fluent 2020R2 [29]. Double-precision option was enabled, once a small error in this case can influence largely the results of the models. For the setup, the energy model was enabled. This model must be activated as this regards the energy related to the temperature change within the combustion process or heat transfer. For the viscous model, as was utilized a step-by-step solution, the first step was made with the realizable k-? and then was used the RSM in the other steps. For the radiation model, the P1 radiation model was chosen to simulate the heat transfer by radiation. This model was chosen for this study because it is accurate enough and reduces the computational cost in relation to the other models. Concerning the species, two models were used. At first to calculate an initial guess, the non-premixed combustion and species transport with one equation were used, for Jet A and hydrogen fuel simulations, respectively. And then, after obtaining a first initial solution converged (or almost converged), the detailed mechanisms referred before (Kundu et al. for Jet A and Li et al. for hydrogen) were imported, and the simulations were resumed until obtaining completely converged solutions. In this case, the used Turbulence-Chemistry Interaction was Eddy-Dissipation and the Chemistry Solver was the Relax to Chemical Equilibrium.

To evaluate the NOx emissions, two approaches were followed. The first one was to use the sub-mechanisms provided in the detailed mechanisms. These sub-mechanisms presented before can cause some problems once; for instance, the sub-mechanism for NOx produced by Jet A does not include the NO_2 species, which clearly will affect the results. The second approach was to use the NOx model provided in ANSYS Fluent. This model must be enabled to ANSYS Fluent display information regarding NOx formation during the solution calculation, or it can be calculated in post-processing (the approach chosen in this work). In the end, an

assessment must be made to reveal which approach is in better agreement with the ICAO's database values (for the Jet A), to be used in the work.

The boundary conditions were defined through an iterative process that has three phases. In the first one, through an iterative process (simulation and result analysis) and the available data present by Ribeiro [28] regarding the conditions of each stage of the GTE (mainly air mass flow, fuel flow, operating pressure, and oxidizer temperature) for 100% power, it was possible to determine the percentage of the air flow that enters the combustion chamber through the swirlers and all the boundary conditions for 100% power.

In phase 2, also through an iterative process (simulation and result analysis), the available data presented by Ribeiro [28] regarding the operating conditions obtained in the test-bed charts presented (mainly the operating pressure and oxidizer temperature), the values of the ICAO's database [12], and the percentage of the air flow that enter the combustion chamber through the swirlers calculated in phase 1, it was possible to define the boundary conditions for 7% power. Finally, after definition the boundary conditions for the conditions of 7% and 100% power, the values of the operating pressure, oxidizer (air) temperature, overall AFR, and primary zone AFR for the other operating conditions were calculated through a linear regression. This allowed the obtention of the boundary conditions for the 30 and 85% power conditions.

Knowing the overall AFR and fuel flow for each condition, it was possible to determine the total air mass flow and then through the primary zone AFR, it is possible to calculate the air mass flow that enters the combustion chamber through the swirlers and the air mass flow that enters through the other entries (mixers and dilution holes). Once these steps were concluded, the boundary conditions for the air mass flow inlets were defined for each power condition of the LTO cycle.

5. Results and discussion

In this section, the results of the simulations are presented. It should be noted that all the results presented are only for one-fourth of the CFM56-3 combustor.

5.1 Combustor exit temperature

The first set of results was obtained during the process of estimation of the boundary conditions where the outlet average static temperatures to the simulations with Jet A fuel were calculated, as shown in **Figure 4**. Those are important values once we need them, first to compare with the reference temperature of 1649.94 K obtained by Ribeiro [28] to the condition of 100% power, and then to get reference values for the outlet temperature to allow the calculation of the mass flow of hydrogen fuel for each power condition.

The quantity of fuel for the simulations with hydrogen was calculated through the mass of Jet A fuel for each power condition and the ratio between the lower heating values, LHV, of the fuels, as shown in Eqs. (13) and (14).

$$\dot{m}_{Hydrogen\ fuel} = \dot{m}_{JetA\ fuel} \times \frac{LHV_{Jet-A}}{LHV_{Hydrogen}} \tag{13}$$

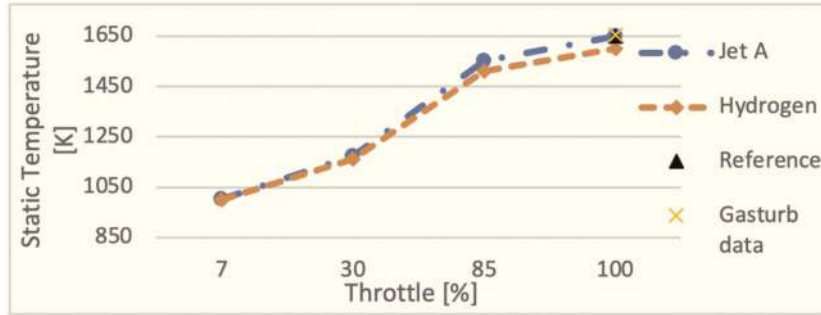$$\dot{m}_{Hydrogen\ fuel} = \dot{m}_{JetA\ fuel} \times 0,3597 \tag{14}$$

Figure 4.
Combustor outlet average static temperature throughout ICAO's LTO cycle, while burning Jet A and Hydrogen fuel; and the reference values for 100% throttle.

Since the LHV changes from author to author, this ratio was calculated and then adjusted for the condition of 7% power in order to get the same value for the outlet average static temperature for the simulations with the Jet A and hydrogen fuel.

Figure 4 shows the most relevant outlet average static temperatures obtained in this work. The values for the sensibility tests are not represented here.

Through **Figure 4** it is possible to conclude that the values of outlet temperature obtained through the simulations with the input data from ICAO and *GasTurb* values (blue line and yellow x, respectively) are quite similar to the reference value for the full power condition (to Jet A).

Through the same figure, but now considering the simulations with hydrogen, it is possible to conclude that:

- The values of outlet temperature for 7% and 30% power are similar to Jet A, which indicates that the ratios between the amount of hydrogen fuel and Jet A must be correct;

- For the conditions of 85% and 100% power, the lower outlet temperature for hydrogen fuel indicates that the quantity of hydrogen should be higher.

In this study, it was opted to fix only one value for the ratio, but as we can see, the best approach seems to be to calculate the specific ratio between the fuels to get the same exact outlet temperatures for each power condition.

5.2 NOx emissions

In the emission analysis, it is possible to study the emissions of all the pollutants, mainly CO, CO_2, UHC, and NOx. However, since in this work the only objective related to the pollutants is to compare the pollutant emissions between the Jet A fuel and hydrogen fuel, the only emissions analyzed were the NOx, once H_2O is not assumed as a pollutant.

Some of the results presented in this section were obtained through the emission index, EI. This value can be obtained using **Eq. (13)**:

$$EI[g/kg] = \frac{\text{Emission flow rate}[kg/s] \times 1000}{\text{Inlet } \dot{m}_{fuel} \ [kg/s]} \tag{15}$$

In **Eq. (13)**, the emission flow rate was obtained by reporting the *Flow rate* of the desired pollutant in the outlet plane in Ansys Fluent, and this value is given in kg/s. The values used for the $\dot{m}_{fuel}$ (obtained from ICAO [12]) at the inlets are given in kg/s. The results are presented in the form g[Emissions]/kg[fuel], which allows the comparison with the ICAO's reference data.

In the first analysis (reference standard), regarding Jet A fuel simulations, the emission index is used since the quantity of fuel burned is the same for each operating condition, and it can be easily interpreted by the reader. However, in the comparison between the pollutant emissions of Jet A fuel and hydrogen fuel, as the quantities of fuel are very different (the mass flow of hydrogen is almost a third of the mass flow of Jet A), the use of the EI may give a wrong perception of the emissions difference to the reader. So, to simplify the analysis, it was opted for the use of the flow rate of NOx, in grams per second, for a fourth of the chamber.

5.2.1 Control simulation and emission comparison between Jet A and hydrogen fuel

The results for the control simulations are presented in **Figure 5a**, which shows the EI(NOx) in the outlet of the quarter of the combustion chamber for the Jet A fuel.

As expected, and previously referred, for both approaches, the NOx emissions are lower at low power settings and attain maximum values at the highest power condition, where the temperatures are higher.

Considering **Figure 5a**, it is possible to conclude that:

• The NOx sub-mechanism clearly overpredicts the NOx quantity, in relation to the reference values (ICAO's database);

• Regarding to the NOx model available in ANSYS Fluent, for the lower power conditions (7 and 30% power), the model can predict values for the NOx
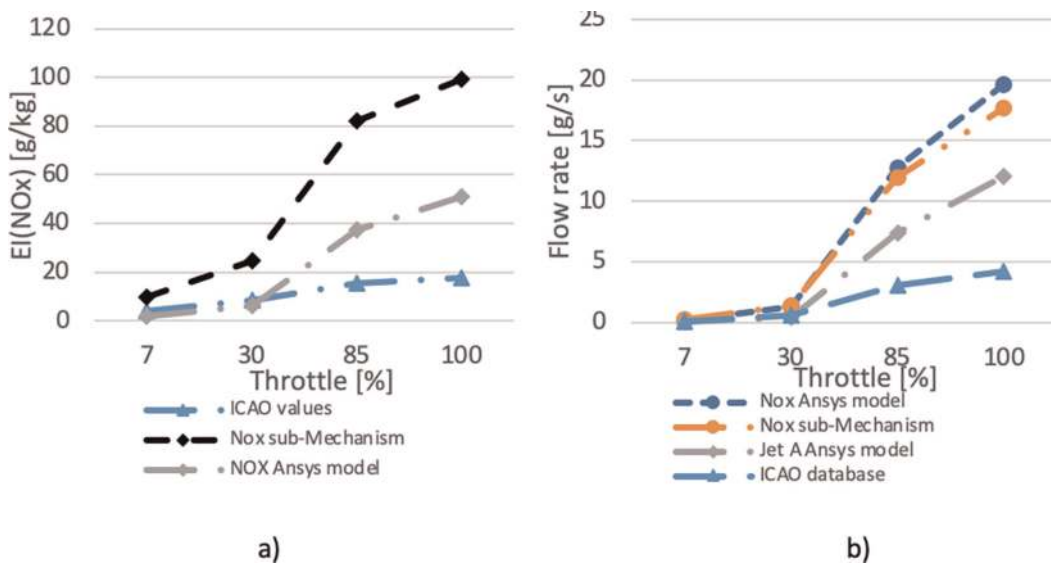

Figure 5.
Results for the NOx emissions for one-fourth of the combustion chamber throughout ICAO's LTO cycle: (a) EI results of NOx for the combustion of Jet A obtained through the use of two approaches, NOx sub-Mechanism and Ansys NOx model; and (b) comparison of the flow rates of NOx for the combustion of Jet A and Hydrogen fuel obtained through the use of two approaches, NOx sub-Mechanism and Ansys NOx model.

quantity close to the ones of ICAO's database; however, for the higher power conditions (85% and 100% power), this model also overpredicts the NOx emissions, in relation to the reference values (ICAO's database), approximately 2.4 times more for 85% power and 2.9 times more for 100% power.

- The NOx model from ANSYS Fluent can predict the NOx emissions better than the other approach, and these values will be used in the next step.

In a second phase, with the same boundary conditions (air mass flow rate, temperature, and pressure) for each operating condition, the simulations were repeated, but now for the hydrogen fuel. **Figure 5b** shows the comparison between the reference values (from ICAO and from the better model of the previous phase for Jet A fuel) and the NOx emission analysis made through two different approaches for hydrogen fuel, the NOx sub-mechanism, and the NOx model from ANSYS Fluent. As referred before, those analyses were made in terms flow rate, with the units of grams per second.

Looking at **Figure 5b**, considering the models used for NOx forecast, it is possible to take two principal conclusions:

- The forecasts made by the ANSYS NOx model provide higher values than those made with the NOx sub-mechanism for all the operating conditions; however, the error between these values is relatively small (up to 10%).

- Comparing the quantity of NOx produced by the hydrogen fuel with Jet A, for the lower power conditions, the quantities of NOx emitted are nearly the double of the values of the Jet A (for both ICAO's database and for the prediction with the model) and for the higher operating conditions, the quantity of NOx emitted continues to be nearly the double of the predicted NOx emissions for the Jet A fuel simulations with the NOx model and the emissions are predicted to be nearly four to five times higher than the reference data from ICAO.

5.2.2 Sensibility tests

In this work, several sensibility tests were carried out, namely the presence of the swirl effect on the swirler's inlets and the influence of the fuel injection pressure and temperature. In this work, the initial value of fuel temperature (used in the study) for the Jet A and the hydrogen fuel was 298.15 K, once this is the fuel temperature used by the software *Gasturb*. The results of these tests are presented in **Figure 6**.

As the represented values are similar, they are also presented in **Table 2**.

About the influence of the swirl effect, whose results for the NOx emissions are presented in **Figure 6a**, if one considers the same forecast approach (only the values of ANSYS model or the values of the sub-mechanism), it is possible to conclude that for this specific case the presence of this phenomenon helps to reduce slightly the quantity of NOx emissions for the high power conditions, while for lower power conditions the NOx values are closer.

To analyze the influence of the inlet fuel temperature, the sensibility tests were made with the hydrogen fuel at 600 K, and the results for the NOx emissions are presented in **Figure 6b**. From this figure, it is possible to conclude that:

- For the simulations with the hydrogen temperature of 600 K, the error between the two approaches used to forecast the NOx is considerable for the higher power
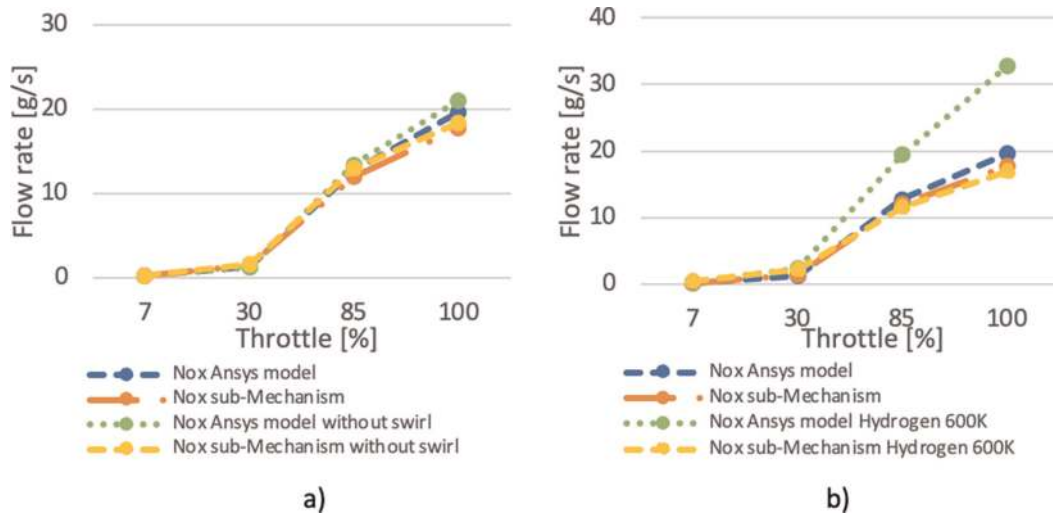
Figure 6.
Flow rates of NOx emissions for the sensibility tests for one fourth of the combustion chamber throughout ICAO's LTO cycle burning hydrogen: (a) analysis of the influence of swirl effect through the use of two approaches, NOx sub-mechanism and Ansys NOx model; and (b) analysis of the influence of the hydrogen fuel temperature through the use of two approaches, NOx sub-mechanism and Ansys NOx model.

Op. Cond.	Standard Reference		Without swirl		Fuel 600 K	
	Sub-Mechanism	*Ansys model*	*Sub-Mechanism*	*Ansys model*	*Sub-Mechanism*	*Ansys model*
100	17.70	19.58	18.30	20.91	16.97	32.70
85	11.97	12.75	12.98	13.40	11.51	19.49
30	1.44	1.30	1.61	1.22	2.26	2.38
7	0.22	0.17	0.24	0.16	0.51	0.32

Table 2.
*NOx flow rates in [g/s] obtained for hydrogen fuel (as in **Figure 6**).*

conditions (85 and 100% power); that is, if we look to the values obtained, the predicted emissions for the NOx model of Ansys are almost twice the value predicted with the NOx sub-mechanism.

- For both approaches, in the lower power conditions (7 and 30% power), the quantity of NOx emitted is higher for the fuel temperature of 600 K than for the reference temperature (298.15 K).

- For the higher power conditions (85 and 100% power), the approaches showed different behavior. For the sub-mechanism, the NOx emissions are lower for the fuel temperature of 600 K and for the NOx model of Ansys, the emissions keep higher than for the reference temperature (298.15 K).

About the injection pressure tests, the modification of this value did not make any changes to the results. For that reason, the results are not presented once they do not allow to analyze the influence of this parameter.

6. Conclusion

In this work, an overview of the use of hydrogen in aviation, the modifications needed to adapt an existent gas turbine to use hydrogen, and a CFD simulation of the CFM56-3 combustor burning hydrogen is provided. During this work, it was demonstrated theoretically that the CFM56-3 can work with hydrogen fuel with minor changes (related only to the injection system).

Regarding the results, starting with the control simulation (reference standard), there are several possible reasons that can be pointed out for the differences between the simulations and the ICAO's database values. For instance, the fact that the fuel was considered in the gaseous state when injected into the combustion chamber simulates "perfect" atomization, increasing the combustion efficiency and creating a higher temperature inside the combustion chamber. Other reason can be the fact that the chosen mechanism/sub-mechanism does not represent the combustion of the Jet A fuel or the NOx production in the best way. The choice of the radiation model can also influence this result, once the radiation representation is more important in the hydrocarbon fuel burn than in the hydrogen fuel burn. Other possible reason could be the chemical model used. However, due to the limited computational resources, it was not possible to use more complex models.

Regarding the other results, comparing the NOx emissions obtained for the simulations (for both Jet A and hydrogen), it was shown that for this geometry of combustor and injector, the quantity of NOx produced when burning hydrogen is almost twice of the NOx emissions for Jet A. Once we are using the same swirlers and injector geometry (single hole) for both fuels, these results are in agreement with the results of C. J. Marek et al. [30], who concluded in their job that using similar injection geometries, the minimum NOx levels for hydrogen fuel were twice than for Jet A fuel.

Finally, regarding the sensibility tests (changing the swirl effect, fuel injection pressure, and temperature), only the changes in swirl effect and the fuel temperature produced relevant changes in the results. The fact that the changes in fuel injection pressure did not produce major changes in the NOx emission results could be explained as the fact that for these tests, the geometry of the injectors was always considered the same (the area of the inlets did not change), and the fuel mass flow rate was the same for each power condition. For that reason, the pressure changes will not affect the behavior of the fuel jet that much. In practice, in gas turbine engines, the pressure is usually used to control the quantity of fuel injected.

Through the results obtained for the tests with the swirl effect, it was demonstrated that without the swirl effect, the NOx emissions increased. After analyzing the recirculation zone (position and form), it was concluded that without the swirl effect, the quality of the recirculation zone was reduced and the temperature across the combustion chamber was slightly increased (also increasing the emissions). So, the presence of the swirl effect helps to stabilize the recirculation zone, reducing the presence of hot spots in the flame.

About the influence of the fuel temperature, it was expected that an exponential raise in this value could affect largely the temperature in the outlet of the chamber, increasing the efficiency. However, that did not happen, and not only the outlet temperature changed just a small percentage (1–2%) for the double of the initial fuel temperature, but also cause malfunctions across the chamber, with greater evidence in the higher power conditions, where the analysis of the flame shows a great deterioration of the recirculation zone and the presence of a phenomenon that seems to be the

occurrence of autoignition or flashback inside the swirlers. These malfunctions were associated with the velocity of hydrogen fuel flow, which has almost doubled when the temperature was raised. The most credible reason for this phenomenon consists of the density reduction of the hydrogen fuel due to that change in temperature.

Acknowledgements

Author details

Rafael Domingues[1] and Francisco Brójo[2]*

1 C-MAST—Center for Mechanical and Aerospace Science and Technologies, Portugal

2 Department of Aeronautical Sciences, University of Beira, Covilhã, Portugal

*Address all correspondence to: brojo@ubi.pt

IntechOpen

References

[1] ICAO (International Civil Aviation Organization). Global environmental trends – present and future aircraft noise and emissions, Working Paper, reference A40-WP/54 EX/21, 5/7/19

[2] ICAO (International Civil Organization). Aviation and the Environment: Outlook, Chapter one in ICAO 2019 Environmental Report, 2019

[3] European Commission. Revision of the EU Emission Trading System Directive 2003/87/EC concerning aviation [Internet], Ref. Ares (2020) 3515933, 03/07/2020. Available from: https://ec.europa.eu/clima/eu-action/transport-emissions/reducing-emissions-aviation_en [Accessed: March 17, 2022]

[4] ICAO (International Civil Organization). Sustainable aviation fuels guide, version 2. 2018

[5] ATAG (Air Transport Action Group). Waypoint 2050 report. Second Ed., September 2021

[6] Brewer GD. Hydrogen Aircraft Technology. Vol. 33431. Boca Raton, Florida: CRC Press; 1991

[7] Seeckt K. Conceptual Design and Investigation of Hydrogen-Fueled Regional Freighter Aircraft, [Licentiate Thesis]. Sweden: Stockholm; 2010

[8] Westenberger A. Hydrogen fuelled aircraft, LAirbus Deutschland GmbH 21129 Hamburg, Germany, 22/05/2003, IN: AIAA 2003-2880

[9] ENABLEH2 [Internet]. Cranfield University; 2022. Available from: https://www.enableh2.eu/ [Accessed: April 25, 2022]

[10] AIRBUS. ZEROe [Internet]. Available from: https://www.airbus.com/en/innovation/zero-emission/hydrogen/zeroe [Accessed: 2022-04-23]

[11] European Aviation Safety Agency. EASA TYPE-CERTIFICATE DATA SHEET -CFM56-2 & CFM56-3 Series Engines. TCDS: E.066, November, 2008

[12] ICAO. ICAO engine exhaust emissions data bank "CFM56-3-B1," Tech. Rep., January. 2015

[13] Aubuchon D, Campbell J. CFM56–3 Turbofan Engine Description. Toronto, Canada: Seneca College; 03/2016

[14] Oliveira J. CFD Analysis of the Combustion of Bio-Derived Fuels in the CFM56-3 Combustor [Master's Thesis]. Covilhã, Portugal: University of Beira Interior; 2016

[15] Mathur ML, Sharma RP. Gas turbines and jet and rocket propulsion. Second ed. Nem Chand Jain, Delhi; 2007

[16] El-Sayed AF. Aircraft Propulsion and Gas Turbine Engines. Second ed. Boca Raton, FL: CRC Press; 2017

[17] Lefebvre AH, Ballal DR. Gas Turbine Combustion. Third ed. Boca Raton, FL: CRC Press; 2010

[18] Morão I. The influence of jet fuels on the emission of pollutants [Master's Thesis]. Covilhã, Portugal: University of Beira Interior; 2019

[19] Lackner M, Winter F, Agarwal AK. Handbook of Combustion: Gaseous and Liquid Fuels. Vol. 3. KGaA, Weinheim: WILEY-VCH Verlag GmbH & Co; 2010. ISBN: 978-3-527-32449-1

[20] Haglind F, Singh R. Design of aero gas turbines using hydrogen. Journal of Engineering for Gas Turbines and Power. 2004;**128**:754-764

[21] Boggia S, Jackson A. Some unconventional aero gas turbines using hydrogen fuel. In: Proceedings of ASME Turbo Expo 2002, Amsterdam. Vol. 2B. New York: ASME; 2002. pp. 683-690

[22] Kuo KK. Principles of Combustion. Second ed. Hoboken, New Jersey: John Wiley & Sons, Inc.; 2005. ISBN 0-471-04689-2

[23] Mostafa, Mohammad Golam, 3D Simulation Of Jet-A Combustion In A Model Aircraft Engine Combustion Chamber. 2012. Theses 90

[24] Kundu K, Penko P, Yang S. Simplified Jet-A/air combustion mechanisms for calculation of Nox emissions. In: Proceedings of the 34th AIAA/ASME/SAE/ASEE Joint Propulsion Conference and Exhibit, Cleveland, Ohio, USA. 1998

[25] Ströhle J, Myhrvold T. An evaluation of detailed reaction mechanisms for hydrogen combustion under gas turbine conditions. International Journal of Hydrogen Energy. 2007;**32**:125-135. DOI: 10.1016/j.ijhydene.2006.04.005

[26] Briones AM, Aggarwal SK. A numerical study of H2–air partially premixed flames. International Journal of Hydrogen Energy. 2005;**30**:327

[27] ANSYS, Inc. 5 Best Practices for Gas Turbine Combustion Meshing Using Ansys Fluent. White Paper. 2020

[28] Ribeiro P. Análise de performance da Família de Motores de Avião CFM56. Master´s Thesis. Lisboa, Portugal: Instituto Superior de Engenharia de Lisboa; 2012

[29] ANSYS, Inc., ANSYS Fluent Theory Guide. Release 2020 R2, July 2020

[30] Marek CJ, Smith TD, Kundu K. Low emission hydrogen combustors for gas turbines using lean direct injection. In: 41st AIAA/ASME/SAE/ASEE Joint Propulsion Conference and Exhibit. Tucson, Arizona, USA. 2005